Dynamic Model of Communicating Hydrocephalus for Surgery Simulation

Olivier Clatz[†*], Stéphane Litrico[‡], Hervé Delingette[†], Philippe Paquis[‡], Nicholas Ayache[†]
[†] Epidaure Research Project, INRIA Sophia Antipolis, France
[‡] Department of Neurosurgery, Hôpital Pasteur, C.H.U. Nice, France
[*] Corresponding author: olivier.clatz@sophia.inria.fr

***Abstract*— We propose a dynamic model of cerebrospinal fluid and intracranial pressure regulation. In this model, we investigate the coupling of biological parameters with a 3D model, to improve the behavior of the brain in surgical simulators. The model was assessed by comparing the simulated ventricular enlargement with a patient case study of communicating hydrocephalus.**

In our model, cerebro-spinal fluid production-resorption system is coupled with a 3D representation of the brain parenchyma. We introduce a new bi-phasic model of the brain (brain tissue and extracellular fluid) allowing for fluid exchange between the brain extracellular space and the venous system. The time evolution of ventricular pressure has been recorded on a symptomatic patient after closing the ventricular shunt. A finite element model has been built based on a CT scan of this patient, and quantitative comparisons between experimental measures and simulated data are proposed.

Keywords: Hydrocephalus, cerebro-spinal fluid, biomechanical model

I. Introduction

Different ventriculostomy surgical simulation systems have been developed in the past years. While only considering the geometry of the brain and visual feedback in their early development stages [1], these systems progressively evolved to incorporate force feedback [2], [3]. However, none of these system are able to simulate properly the behavior of the brain and its interaction with the cerebro-spinal fluid. We believe the lack of biological relevance of these simulators is a major restriction towards their adoption for training of surgeons.

We propose a dynamic model of cerebrospinal fluid and intracranial pressure regulation, coupling a volumetric biomechanical model with a scalar representation of the CSF circulation. The mathematical simplicity of the interaction of CSF with brain in this model makes it adequate for integration in a real time surgical simulation system.

Three main components influence ICP: CSF production, circulation, and drainage. The normal CSF dynamics can be described as follow: CSF is mainly produced by the choroid plexus in the lateral and third ventricles. The CSF then flows along the aqueduct of Sylvius, into the fourth ventricle, then through the lateral foramina of Luschka and the medial foramen of Magendie to reach the subarachnoid space. CSF resorption takes place through arachnoid granulations in the sagittal sinus.

High intraventricular pressure hydrocephalus (as opposed to normal pressure hydrocephalus) are pathological states encountered when CSF circulation or drainage is modified. *Communicating* hydrocephalus is characterized by the obstruction of CSF in the sub-arachnoid space.

Mathematical models of CSF hydrodynamics found in the literature can be classified into two categories: scalar and spatial (2D and 3D) models (see Section II-A). Scalar models [4]–[6] have been used to quantify the CSF outflow resistance or the pressure-volume index.

To the best of our knowledge, current spatial models [7], [8] have only considered non-communicating hydrocephalus. These models assume a pressure gradient in the parenchyma. However, recent experimental studies tend to demonstrate that this hypothesis may not be valid [9], [10].

Subarachnoid hemorrhage is the presence of blood within the subarachnoid space, which affects the CSF outflow resistance. As a consequence, the pressure of CSF increases, and ventricles enlarge. Our model has been used to simulate hydrocephalus: the temporal evolution of brain deformation and ventricular pressure after closing the shunt are computed. Model parameters have been estimated based on a retrospective case study with pressure measures and images. A quantitative evaluation of the residual error is proposed.

II. Hydrocephalus Models

A. Literature Review

1) Scalar Models: The first representation of the cerebral hydrodynamics was done by Monroe [11] and modified by Kellie [12]. The Monroe-Kellie doctrine simply assumes that the brain, CSF, and blood are enclosed within a rigid shell, so that any increase in volume of one of the compartments implies a decrease of the others. In 1972, Guinane [4] proposed an equivalent circuit analysis of CSF hydrodynamics (Figure 1). This system is governed by the following differential equation:

$$C\frac{\partial P}{\partial t} + \frac{P}{R_1} = Q_1 + \frac{P_D}{R_1} \tag{1}$$

P is the CSF pressure inside the ventricles. C is a constant that describes the relationship between the volume V_{CSF} and the pressure P in the ventricles: $C(P) = \partial V_{CSF}/\partial P$. R_1 is the CSF absorption resistance. Q_1 is the flow rate of CSF

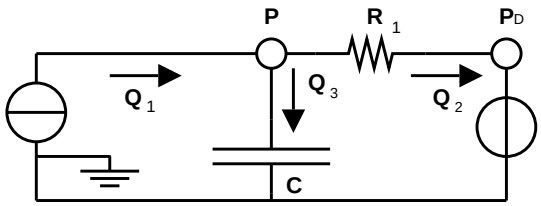

Fig. 1. Equivalent circuit analysis of CSF hydrodynamics proposed by Guinane [4]. The symbol ⊖ represents a perfect flow supply (constant CSF production rate in the choroid plexus). The symbol ⊕ stands for a perfect pressure supply (constant the sagittal sinus pressure).

produced in the choroid plexus. P_D is a threshold pressure under which the absorption stops (usually taken as the sagittal sinus pressure).

The successive updates of this model mainly consisted of improving the relationship $\partial V_{CSF}/\partial P$, the influence of which is major on the dynamic behavior of the model. Recently, Sivaloganathan *et al.* [5] showed that any model based on a two compartment assumption (brain and CSF) can be derived from Equation 1 using an appropriate pressure-volume (P-V) relationship $C\,(P)$.

The two-compartment model has only recently been modified to add several additional compartments. In 2000, Stevens *et al.* [6] proposed a four-compartment model that included the rest of the body.

2) Spatial Models: An alternative to the scalar models was proposed by Nagashima *et al.* [7] in 1987 to model a non-communicating hydrocephalus. His 2D model was based on the linear consolidation theory of Biot [13], discretized with the finite element method (FEM). In the linear consolidation theory, the brain is approximated as an elastic porous medium containing CSF in the extracellular space. The CSF flow is then described by Darcy's law:

$$n\left(\underline{v_f}-\underline{v_s}\right)+\underline{\underline{K}}\,\underline{\nabla p}=0 \tag{2}$$

Where n is the porosity, $\underline{v_f}$ and $\underline{v_s}$ are respectively, the velocities of the fluid and the solid phases (m s^{-1}), $\underline{\underline{K}}$ is the hydraulic permeability (m^4 N^{-1} s^{-1}), and p is the interstitial fluid pressure (N m^{-2}).

The authors propose to impose a pressure gradient between the ventricles and the cortex as a boundary condition, inducing (as a consequence of Darcy's law, Equation 2) a CSF flux through the brain parenchyma. Note that in this model, the CSF and the extracellular brain fluid are a single phase.

The work of Nagashima *et al.* has been later extended by Peña *et al.* [8] to the study of local measures (void ratio, effective stress, stretch), also on a 2D model.

Recently, the elastic modulus of the brain parenchyma in the biphasic model has been revised by Taylor *et al.* [14]: closer to 600 Pa rather that in the range (3-100 kPa), as proposed in previous studies.

B. Proposed Model

1) Introduction: The weakness of scalar models resides in their inability to describe the expansion of the ventricular wall, or the collapse of the ventricles upon insertion of a shunt. Up to now, the spatial models could not include CSF production and resorption phenomena as boundary conditions.

We propose a new model of communicating hydrocephalus, combining a 3D patient-specific biphasic model of the brain with a scalar description of the CSF production-resorption cycle. We consider the two-compartment model (brain and CSF), and introduce the spatial finite element model to compute the pressure volume relationship.

In this model, the CSF is free to flow through the aqueduct of Sylvius, which is not obstructed. The circulation of CSF through the brain parenchyma and the ventricular wall is thus neglected. The CSF pressure P is different from the brain interstitial fluid pressure p, and the ventricular wall displacement is determined by the effective pressure $P^* = P - p$ on the ventricular wall.

Because the amount of fluid flowing through the brain is very limited in communicating hydrocephalus, we neglect the viscosity of the interstitial fluid, and the pressure gradient induced by Darcy's law 2. Nevertheless, we allow for interstitial fluid exchange with blood through the blood-brain barrier (BBB).

2) Formulation:

a) Spatial Model: We consider the brain to be a biphasic material, composed of an elastic matrix (the brain tissue) and interstitial fluid (the extracellular fluid) obeying the following quasi-static linear elastic laws:

$$\underline{\underline{\epsilon}}=\frac{1}{2}\left(\underline{\underline{\nabla u}}+\underline{\underline{\nabla u}}^T\right) \qquad \text{Strain tensor definition} \tag{3}$$

$$\underline{\underline{\sigma_s}}=\lambda\, tr(\underline{\underline{\epsilon}})+2\,\mu\,\underline{\underline{\epsilon}} \qquad \text{Constitutive equation} \tag{4}$$

$$\underline{\underline{\sigma}}=\underline{\underline{\sigma_s}}+p\,\underline{\underline{I_3}} \qquad \text{Stress tensor definition} \tag{5}$$

$$div\left(\underline{\underline{\sigma}}\right)+\underline{f}=0 \qquad \text{Equilibrium equation} \tag{6}$$

Variables and parameters are defined in Table I. In this paper, we consider the Young's modulus, E, and Poisson's ratio, ν, to characterize the material. λ and μ are the Lamé coefficients, computed as simple functions of E and ν (see [15]).

Symbol	Quantity	Unit
$\underline{\underline{\epsilon}}$	Strain tensor	
$\underline{u}$	Displacement of the solid phase	m
$\underline{\underline{\sigma_s}}$	Effective stress (solid phase)	Pa
λ & μ	Lame elastic & shear modulus	Pa
$\underline{\underline{\sigma}}$	Total stress	Pa
p	Fluid pressure	Pa
$\underline{f}$	External volumetric forces	N m^{-3}

TABLE I
VARIABLE AND PARAMETER DEFINITION.

In communicating hydrocephalus, the CSF production-resorption cycle is comparable to the cycle described in Section I for the healthy subject, but the hydraulic absorption resistance in the venous system is increased as a consequence of the subarachnoid hemorrhage. The CSF flows through the aqueduct of Sylvius and CSF drainage through the brain is minimal. Thus we propose to neglect the viscous effect of fluid motion in the brain matrix, leading to a constant interstitial

pressure, p, in the brain. As a consequence:

$$div\,(p) = 0 \text{ in the brain volume} \quad (7)$$

$$\underline{\underline{\sigma}}.\underline{n} + p = P \text{ on the ventricular wall} \quad (8)$$

Where $\underline{n}$ is normal to the ventricle surface.

In addition, we allow for fluid exchange between the interstitial space and the blood capillaries in the brain, through the BBB (otherwise, brain could not deform since the interstitial fluid is incompressible). This absorption flow is considered linear with the pressure difference between the extracellular space and the capillary pressure. The BBB hydraulic resistance is modeled by R_2:

$$\frac{\partial V_{brain}}{\partial t} + \frac{1}{R_2}(p - P_D) = 0 \quad (9)$$

b) Scalar Model: The CSF circulation in the intracranial space is described by the general two-compartment model, obeying the differential equation:

$$\frac{\partial V_{CSF}}{\partial t} + \frac{P}{R_1} = Q_1 + \frac{P_D}{R_1} \quad (10)$$

c) Combined Model: The first term of Equation 10 can be decomposed as: $\frac{\partial V_{CSF}}{\partial t} = \frac{\partial V_{CSF}}{\partial P^*}\frac{\partial P^*}{\partial t}$. Using this formulation, the derivative of the volume of the ventricles with respect to the effective pressure $\partial V_{CSF}/\partial P^*$ can be computed using the FEM. The mechanical model presented in Section II-B.2.a is thus used to discretize the relation between the volume of the ventricles and the effective pressure. The system can then be expressed as an ordinary differential equation (see [15] for intermediate calculus):

$$\frac{\partial V_{CSF}}{\partial P^*}\left(1 + \frac{R_2}{R_1}\right)\frac{\partial P}{\partial t} + \frac{1}{R_1}P = Q_1 + \frac{P_D}{R_1} \quad (11)$$

3) Boundary Conditions and Integration Method: The FEM has been used to pre-compute $\partial V_{CSF}/\partial P^*$: the outer surface of the mesh (cortex) is fixed, and we set the pressure P^* in the ventricles. The use of pre-computation for the mathematical problem enables real time update of the model position at 200Hz on a Pentium M 760 laptop (see [15] for details on the numerical scheme). The low complexity associated with the coupling of the proposed 3D model with a first order ordinary differential equation makes it also adapted for integration with other numerical integration schemes.

III. Evaluation: Case Study

A. Acquired measures

The simulation is based on a retrospective case study: the patient was a 45 years-old woman presenting a subarachnoid haemorrhage induced by an aneurysm rupture. An external ventricular shunt with a pressure probe was inserted. CSF pressure was recorded during a shunt closure. Two control CAT scan were acquired before and after closing the shunt. The CSF production rate was also recorded every hour (shunt reservoir at ventricles level).

Pressure was recorded 48 hours after shunt insertion. The pathology, characterized by the value of R_1, had already evolved: the steady state pressure after closing the shunt was 1066 Pa (8 mmHg) lower than the pressure measured immediately after shunt insertion.

B. Geometric model

The brain and ventricles of the patient were segmented in the images with classical mathematical morphology operations. This segmentation has been meshed with tetrahedra using a state of the art meshing software [16] (17 ,000 vertices, 200 ,000 tetrahedra). The third and fourth ventricles were too collapsed in the image to be segmented, so that we made the assumption that only the lateral ventricles deform. However, there is no limitation in the proposed method to their inclusion in the simulation.

C. Identification of Parameters

The unknowns of our system are R_1, R_2, P_D, Q_1, E, and ν. Two of these parameters are assumed to be constant among patients and are taken from the literature: the sagittal sinus pressure, $P_D = 906$ Pa (6.8 mmHg) [6], and the Poisson's ratio of the brain, $\nu = 0.35$ [14]. Q_1 is directly measured on the graduated reservoir of the shunt every hour. We measured an average CSF production rate $Q_1 = 16$ ml/h. R_1 is computed from the steady state pressure, P_∞, after closing the shunt: $R_1 = (P_\infty - P_D)/Q_1$. To estimate E, we minimize the closest distance $\underline{d}$ between (i) the simulated steady position of the ventricles and (ii) the position of the ventricles observed on the CAT image, using a Powell algorithm. The Young's modulus E is then defined as the value that minimizes the sum of this squared distance on the overall ventricular surface Ω:

$$\arg\min_E \int_\Omega \|\underline{d}\|\, d\Omega \quad (12)$$

Finally, the value of R_2 is also estimated with a Powell algorithm, minimizing the squared difference between the simulated pressure evolution and the measured pressure in the ventricles. The computed values are given in table II.

Variable	Value
P_D	906 Pa
P_∞	1729 Pa
ν	0.35
E	7221 Pa
Q_1	16 ml.h^{-1}
R_1	51 Pa.ml^{-1}.h
R_2	16 Pa.ml^{-1}.h

TABLE II
VARIABLE VALUES.

D. Simulation of the Enlargement of the Ventricles

We used the model to simulate the progressive enlargement of ventricles after closing the CSF shunt. In this section, we evaluate and discuss the residual error after optimization of the parameters.

First, the displacement error of the ventricle surface was estimated based on the CT scan of the patient and the mesh. The average displacement of the ventricle surface is 2 mm, and the average error computed by the model is 0.8 mm, which is an average relative error of 40%. Figure 3 shows the distribution of this error on the surface of the ventricles. As we can see, the error mainly occurs in high curvature areas, in the occipital horn of the ventricles, where the ventricles do

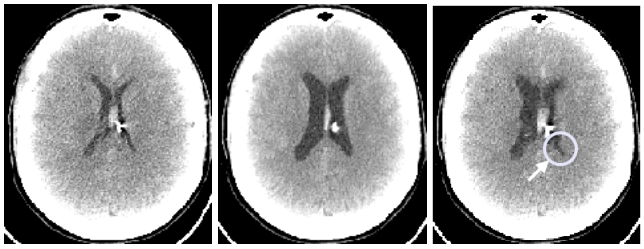

Fig. 2. CT scan of the patient in (left) opened shunt configuration, acquired 1 hour after the procedure and (middle) closed shunt configuration, acquired 48 hours after the procedure (steady state). (right) simulated CT scan after model-computed ventricular enlargement (steady state).

not deform enough. This is also confirmed on Figure 2 (circled area).

Second, we examined the squared difference between the measured time evolution of the ventricular pressure in the patient and the simulated pressure evolution (Figure 3). The average error on measure points is 9%, with a maximum error of 16.2% (60 minutes after closing the shunt).

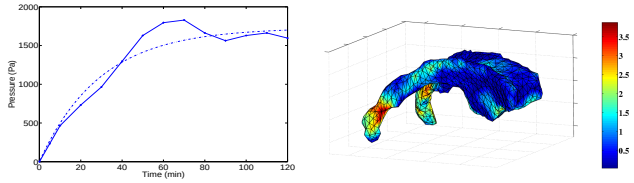

Fig. 3. Evaluation of the simulation. Left: evolution of the ventricular pressure as a function of time after closing the shunt. Continuous line: Measure on the patient. Dashed line: Simulated pressure increase with the model. Right: distribution of the displacement error on the ventricle surface mesh (mm).

E. Discussion

The error criteria and the mesh are based on segmentations of the ventricles. This makes them sensitive to segmentation error. In particular, if the ventricles are very contracted, as on the open shunt configuration image (left panel of Figure 2), part of the ventricle can be missed by the segmentation leading to the undeformed part of the ventricle (circled area in right panel of Figure 2).

The linearity of the model may show some limitations in the horn of the ventricles. This error source can be of even greater importance for patient with more acute hydrocephalus. In addition, the influence of blood vessels and in particular auto-regulation in the brain might be able to explain the rebound observed on the pressure to time evolution (Figure 3).

A higher time sampling (every minute) would also allow to capture transient phenomena. Ideally, an automatic system should be used to record this pressure.

IV. Conclusion

We proposed in this article a new model of hydrocephalus, which couples a 3D representation of the brain parenchyma with a scalar hydraulic description of the CSF circulation in the intracranial space. The link between the scalar and the 3D model has been made through the relation $\partial V_{CSF}/\partial P^*$, which makes this model amenable to further improvements, either of the mechanical constitutive equation (including a non linear relation, for example), or of the scalar model (incorporating additional electric equivalent components).

The current model revokes the assumption that the brain is incompressible, and allows for brain extracellular fluid exchange with the blood. Contrary to previous spatial models, our model does not assume that CSF is drained through the brain. As a consequence, we make the assumption that interstitial fluid viscosity can be neglected, leading to a brain pressure in agreement with the recent in-vivo measurements [9], [10].

The evaluation of the model shows a realistic behavior, both in terms of pressure and deformation simulation. The mathematical simplicity of the model -linear elasticity and ordinary differential equation for the CSF circulation- makes its suitable for fast computation and integration in a surgical surgery simulator.

References

[1] N. I. Phillips and N. W. John, "Web-based surgical simulation for ventricular catheterization," *Neurosurgery*, vol. 46, no. 4, pp. 933–936, Apr 2000.

[2] B. Panchaphongsaphak, D. Stutzer, E. Schwyter, R. L. Bernays, and R. Riener, "Haptic device for a ventricular shunt insertion simulator," *Stud Health Technol Inform*, vol. 119, pp. 428–430, 2005.

[3] C. Luciano, P. Banerjee, G. M. Lemole, and F. Charbel, "Second generation haptic ventriculostomy simulator using the immersivetouch(tm) system," *Stud Health Technol Inform*, vol. 119, pp. 343–348, 2005.

[4] J. Guinane, "An equivalent circuit analysis of cerebrospinal fluid hydrodynamics." *Am J Physiol.*, vol. 223, no. 2, pp. 425–30, Aug 1972.

[5] S. Sivaloganathan, G. Tenti, and J. M. Drake, "Mathematical pressure volume models of the cerebrospinal fluid," *Appl. Math. Comput.*, vol. 94, no. 2-3, pp. 243–66, 1998.

[6] S. Stevens and W. Lakin, "Local compliance effects on the global csf pressure-volume relationship in models of intracranial pressure dynamics." *Mathematical and Computer Modeling of Dynamical Systems*, vol. 6, no. 4, pp. 445–465, 2000.

[7] T. Nagashima, N. Tamaki, S. Matsumoto, B. Horwitz, and Y. Seguchi, "Biomechanics of hydrocephalus: A new theoretical model." *Neurosurgery*, vol. 21, no. 6, pp. 898–904, 1987.

[8] A. Peña, M. Bolton, H. Whitehouse, and J. Pickard, "Effects of brain ventricular shape on periventricular biomechanics: A finite-element analysis." *Neurosurgery*, vol. 45, no. 1, pp. 531–538, 1999.

[9] H. Stephensen, M. Tisell, and C. Wikkelso, "There is no transmantle pressure gradient in communicating or noncommunicating hydrocephalus," *Neurosurgery*, vol. 50, no. 4, pp. 763–771, Apr 2002.

[10] R. D. Penn, M. C. Lee, A. A. Linninger, K. Miesel, S. N. Lu, and L. Stylos, "Pressure gradients in the brain in an experimental model of hydrocephalus," *J Neurosurg*, vol. 102, no. 6, pp. 1069–1075, Jun 2005.

[11] A. Monroe, "Observations on the structure and function of the nervous system." Creech & Johnson, Edinburgh, 1783.

[12] G. Kellie, "An account of the appearances observed in the dissection of two of three individuals presumed to have perished in the storm of the 3d, and whose bodies were discovered in the vicinity of leith on the morning of the 4th of november 1821 with some reflections on the pathology of the brain." *Trans Med Chir Sci Edinb*, no. 1, pp. 84–169, 1824.

[13] M. Biot, "General theory of three-dimensional consolidation." *Journal of Applied Physics*, no. 12, pp. 155–164, 1941.

[14] Z. Taylor and K. Miller, "Reassessment of brain elasticity for analysis of biomechanisms of hydrocephalus," *Journal of Biomechanics*, vol. 37, no. 8, pp. 1263–1269, Aug 2004.

[15] O. Clatz, S. Litrico, H. Delingette, and N. Ayache, "Dynamic model of communicating hydrocephalus for surgery simulation," INRIA, Research Report 5934, 06 2006. [Online]. Available: https://hal.inria.fr/inria-00080553

[16] S. Oudot, L. Rineau, and M. Yvinec, "Meshing volumes bounded by smooth surfaces," INRIA, Research report 5626, 2005.